
Green Hierarchical Vision Transformer for Masked Image Modeling

Lang Huang¹, Shan You^{2*}, Mingkai Zheng³, Fei Wang², Chen Qian², Toshihiko Yamasaki¹

¹The University of Tokyo; ²SenseTime Research; ³The University of Sydney

{langhuang,yamasaki}@cvm.t.u-tokyo.ac.jp

{youshan,wangfei,qianchen}@sensetime.com, mzhe4001@uni.sydney.edu.au

Abstract

We present an efficient approach for Masked Image Modeling (MIM) with hierarchical Vision Transformers (ViTs), *e.g.*, Swin Transformer [43], allowing the hierarchical ViTs to discard masked patches and operate only on the visible ones. Our approach consists of two key components. First, for the window attention, we design a Group Window Attention scheme following the Divide-and-Conquer strategy. To mitigate the quadratic complexity of the self-attention w.r.t. the number of patches, group attention encourages a uniform partition that visible patches within each local window of arbitrary size can be grouped with equal size, where masked self-attention is then performed within each group. Second, we further improve the grouping strategy via the Dynamic Programming algorithm to minimize the overall computation cost of the attention on the grouped patches. As a result, MIM now can work on hierarchical ViTs in a **green** and efficient way. For example, we can train the hierarchical ViTs about $2.7\times$ faster and reduce the GPU memory usage by 70%, while still enjoying competitive performance on ImageNet classification and the superiority on downstream COCO object detection benchmarks.[†]

1 Introduction

Driven by the great success of Masked Language Modeling (MLM) [50, 51, 13, 5] in natural language processing (NLP) and the advancement of Vision Transformer (ViT) [15, 43, 60, 69], Masked Image Modeling (MIM) emerged as a promising self-supervised pre-training paradigm for computer vision (CV). MIM learns representations from unlabelled data by masked prediction, *e.g.*, predicting the discrete tokens [2], the latent features [73, 62, 1], or the raw pixels [22, 66] of the randomly masked input image patches. Among them, the representative work Masked Autoencoder (MAE) [22] exhibited competitive performance as well as impressive efficiency. In essence, MAE proposed an asymmetric encoder-decoder architecture for MIM, where the encoder (*e.g.*, a standard ViT model [15]) operates only on visible patches, and the light-weight decoder recovers all patches for mask prediction.

On the one hand, the asymmetric encoder-decoder architecture significantly reduces the computation burden of pre-training. On the other hand, MAE only supports the isotropic ViT [15] architecture as the encoder, while most of the modern vision models adopt hierarchical structure [37, 25, 43], in part due to the need of handling the scale-variations of visual elements. In fact, the hierarchical structure and local inductive bias are crucial in various CV tasks that require representations of different levels or scales to make predictions, including image classification [25], and object detection [19]. Yet it is still not straightforward how the hierarchical vision transformers, *e.g.*, Swin Transformer [43], can be integrated into the MAE framework. Moreover, though the work SimMIM [66] has explored

*Corresponding author. [†]Code and pre-trained models: <https://github.com/LayneH/GreenMIM>.

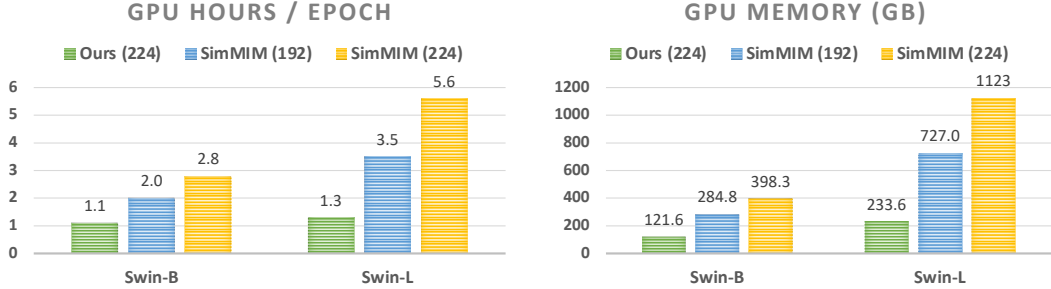


Figure 1: **Comparison with SimMIM in terms of efficiency.** All methods use a Swin-B/Swin-L backbone and batch size of 2,048. The experiments of our method are conducted on a single machine with eight V100 GPUs, CUDA 10, and PyTorch 1.8, while those of SimMIM require 2 or 4 machines.

Swin Transformer for MIM, it operates on both visible and masked patches and suffers from heavy computation costs compared with MAE. As a concrete example, we find that even the base size model of SimMIM cannot be trained on a single machine with eight 32GB GPUs, let alone the larger ones. The computation burden makes it difficult for a wider range of researchers to dive into this field of research, not even to mention the amount of carbon emission during the model development process.

To this end, we strive to devise a new and green approach for MIM with hierarchical models, in the spirit of **Green AI** [55, 67]. Our work focuses on extending the asymmetric encoder-decoder architecture of MAE to hierarchical vision transformers, particularly the representative model Swin Transformer [43], for the sake of efficient pre-training on visible patches only. We identify that the major obstacle is the limitation of the local window attention. Though widely used in hierarchical vision transformers, the local window attention does not work well with the random masking as it creates various-sized local windows that are infeasible for computing in parallel.

This paper provides the first attempt to address this drawback. Our methodology is conceptually simple and consists of two components. First, guided by the Divide-and-Conquer principle, we present a Group Window Attention scheme first partitioning the local windows with uneven numbers of visible patches into several equal-sized groups and then applying the masked attention within each group. Second, we formulate the aforementioned group partition as a constrained optimization problem, where the objective is to find a group partition that minimizes the computation cost of the attention on the grouped tokens. Inspired by the concept of Dynamic Programming [4] and the greedy principle, we propose an Optimal Grouping algorithm that adaptively selects the optimal group size and partitions the local windows into a minimum number of groups. Our methodology is generic and does not make *any* modification to the architecture of the backbone models, such that we can make apple-to-apple comparisons with the baseline operating on both visible and masked patches. In our experimental evaluation, we observed that our method requires substantially less training time and consumes much less GPU memory while performing on par with the baseline. Concretely, using Swin-B [43], our method requires only half of the training time and about 40% of GPU memory consumption compared with the baseline SimMIM, while achieving 83.7% top-1 fine-tuning accuracy on the ImageNet-1K [54] that is on par with SimMIM.

Our contributions. We make the following main contributions:

1. We design a **Green** Hierarchical Vision Transformer for Masked Image Modeling that advocates a more practical method with drastically improved efficiency.
2. As shown in Figure 2, we present a Group Window Attention scheme, gathering the local windows with different numbers of visible patches into several equal-sized groups and then applying the masked attention within each group (see Figure 3).
3. Inspired by the concept of Dynamic Programming [4] and the principle of the greedy algorithm, we propose an Optimal Grouping algorithm (see Algorithm 1) that adaptively selects the optimal group size and partitions the local windows into the minimum number of groups.
4. Extensive experimental evaluations on the ImageNet-1K [54] and the MS-COCO [41] datasets demonstrate that our method can obtain comparable performance to the baselines with more than $2\times$ efficiency improvement (see Figure 1, Tables 2 and 3).

2 Related Works

Self-Supervised Learning. Representation learning is a long-standing and fundamental question in CV. For a long time, representation learning had been dominated by supervised learning. Until recent three years, self-supervised learning (SSL) exhibited impressive performance and attained significant attention. Generally, SSL solves a proxy task without the actual interest to learn good representations. According to the proxy tasks, SSL methods can be categorized into generative approaches and discriminative approaches. Generative approaches predict the original data based on the partially observed inputs [59, 49, 38], predict the transformation applied to the input [46, 18], or model pixels in the input space [36, 20, 33, 27]. Masked Image Modeling also falls into this category. Discriminative approaches received more interest during the past few years, especially the contrastive learning methods. Contrastive learning creates multiple views of images with a set of random data distortions and encourages the representations to be invariant to the distortions. A large number of contrastive learning approaches [63, 47, 23, 9, 71, 72] drive the training by maximizing the similarities between positive samples (*i.e.*, views from the same image) while minimizing those between the negative samples, and some works simply get rid of the negative pairs [21, 6, 10, 31, 70, 7]. Beyond contrastive learning on global features, several methods proposed to maintain the spatial information of representations and use region/mask/pixel-level contrastive learning [61, 65, 64, 26, 29].

Masked Language/Image Modeling. Self-supervised pre-training has revolutionized the NLP. Among them, the Masked Language Modeling (MLM) proposed in BERT [13] and its variants [5] are the most dominant methods, which learn representations by predicting the tokens that are randomly masked in the input sentence. Masked Image Modeling has a similar idea of predicting corrupted images, and some of these methods [59, 49] were proposed Even preceded to BERT. These methods were, however, unable to perform on par with other pre-training paradigms at that time. Until recently, aided by the significant advancement of Vision Transformers [15], several MIM methods presented promising results [15, 2, 22, 66, 62] and became the state-of-the-art of self-supervised learning in CV. These methods can be roughly differentiated in terms of the prediction target, *e.g.*, color bins [15], discrete tokens [2, 14] from pre-trained VAEs [57, 52], raw pixels [22, 66], and handcrafted features [62]. Among these approaches, MAE [22] exhibited competitive performance as well as impressive efficiency as it discards the masked tokens and operates only on the visible ones.

Isotropic and Hierarchical Vision Transformers. The seminal work Vision Transformer (ViT) [15] revolutionized the conventional view of images. ViT, and its variants [56], treat an image as a sequence of patches and adopt a pure Transformer [58] backbone to model the patches for image classification, achieving an impressive performance even compared with the Convolutional Neural Networks. Nevertheless, while the results of ViT are promising in classification, its performance on dense prediction tasks is less favorable, which is largely due to its low-resolution feature maps inherited from its isotropic structure and the quadratic complexity of self-attention [58]. To this end, a strand of works proposed hierarchical structure [60, 43, 16, 69] and efficient attention [30, 43, 12, 32] for ViTs, unleashing the potential of ViTs as general-purpose vision backbones. Our work performs studies upon the representative method Swin Transformer [43] with (shifted) window local attention that is also widely adopted in other methods [12, 69, 32].

Green AI. Witnessing the exponential growth of computations of big AI models [13, 5, 42], the concept of **Green AI** attains mounting attention in recent years [55, 67]. Rather than being merely obsessed with accuracy, **Green AI** advocates making efficiency an important measure of AI models, championing the greener approaches that are more inclusive to the research community. This work follows the path of **Green AI** and presents a greener approach for MIM with hierarchical ViTs.

3 Approach

3.1 Preliminary

Notations. Let $\mathbf{X} \in \mathbb{R}^{C \times H \times W}$ denote the input feature where C , H , and W are the numbers of channels, height, and width of \mathbf{X} ; $\mathbf{M} \in \{0, 1\}^{H \times W}$ denotes the (spatial) mask generated randomly during training where 0 indicates a patch is invisible for the encoder, and vice versa.

Masked Image Modeling. MIM learns representations by predicting the masked portion of a input \mathbf{X} from its partial observation $\hat{\mathbf{X}} \leftarrow \text{Mask}(\mathbf{X}, \mathbf{M})$. Existing MIM methods fall into two categories

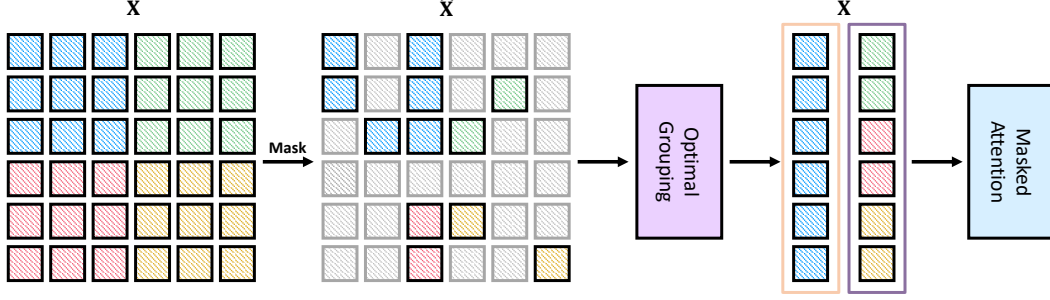


Figure 2: **Illustration of the Group Window Attention scheme.** In Masked Image Modeling (MIM), the input \mathbf{X} , where different colors indicate the tokens belong to different local windows, is randomly masked, producing $\hat{\mathbf{X}}$ of which most tokens are invisible. Our Group Window Attention first performs an optimal grouping to group the visible tokens of the local windows into several equal-sized groups, forming $\bar{\mathbf{X}}$. Finally, we perform the Masked Attention within each group to ensure no inter-window information leakage.

regarding the $\text{Mask}(\cdot, \cdot)$ operation. Most methods [2, 66, 62] use the Hadamard product for masking and retain the masked patches, *i.e.*, $\hat{\mathbf{X}} \leftarrow \text{Mask}(\mathbf{X}, \mathbf{M}) = \mathbf{X} \odot \mathbf{M}$ with \mathbf{M} broadcasted for C times along the channel dimension. In sharp contrast to these methods, Masked Autoencoders (MAE) [22] proposes throwing the masked patches at the masking stage, *i.e.*,

$$\hat{\mathbf{X}} \leftarrow \text{Mask}(\mathbf{X}, \mathbf{M}) = \{\mathbf{X}_{i,j} : \mathbf{M}_{i,j} = 1\}. \quad (1)$$

MAE designs an asymmetric and isotropic encoder-decoder architecture to take advantage of partial inputs: the encoder operates only on the visible patches $\hat{\mathbf{X}}$ without mask tokens; the decoder reconstructs the original images from representations of visible patches and masked tokens. This design allows MAE to achieve competitive performance as well as impressive efficiency, *e.g.*, $3\times$ training speedup compared with the ones operating on all patches. Nevertheless, the MAE works only with the isotropic ViTs and it is unclear *how to translate the efficiency of MAE to hierarchical ViTs*, which exhibited nearly unanimous superiority over the isotropic ones on most vision tasks [60, 43, 16, 12, 69]. In this paper, we attempt to answer this question and propose a much **greener** approach for MIM with Hierarchical ViTs.

3.2 Green Hierarchical Vision Transformer for Masked Image Modeling

Base architecture. We choose the representative hierarchical Vision Transformer–Swin Transformer [43]–as our baseline, which mainly consists of the Feed-Forward Networks (FFNs) and the (shifted) window attentions. While the FFNs are point-wise operations and can operate only on the visible patches, the window attentions fail to do so. Given a window size p (*e.g.*, 7 for Swin), window attention first partitions the feature map \mathbf{X} into $n_w = \frac{H}{p} \times \frac{W}{p}$ non-overlapped local windows as $\mathbf{X} \rightarrow \{\mathbf{X}_i\}_{i=0}^{n_w}$ where each \mathbf{X}_i contains $p \times p$ patches. Then the Multi-head Self-Attention (MSA) [58] is performed within each window independently in parallel because each window contains the same number of patches. Nevertheless, when the numbers of patches within the local windows are uneven, *i.e.*, due to the random masking as in Figure 2, it is unclear how to efficiently compute the attention in parallel. To this end, we propose an efficient Group Window Attention scheme and directly replace all (shifted) window attentions in Swin to make it operate only on visible patches in a **green** manner.

Group Window Attention. Regarding the aforementioned problem, we propose a Group Window Attention scheme that significantly improves the computation efficiency of window attention on masked features. Given the masked feature $\hat{\mathbf{X}} = \text{Mask}(\mathbf{X}, \mathbf{M})$ following Equation (1), we collect a set of uneven local windows $\hat{\mathbf{X}} \rightarrow \{\hat{\mathbf{X}}_i\}_{i=0}^{n_w}$ of which each element contains the visible tokens only, with sizes $\{w_i\}_{i=0}^{n_w}$ accordingly. As shown in Figure 2, our Group Window Attention first uses an Optimal Grouping algorithm to partition the uneven windows into several equal-sized groups and then perform Masked Attention within each group to avoid information leakage. In the next two subsections, we will elaborate on these two components, respectively.

Algorithm 1 Optimal Grouping

Require: The number of visible patches within each local window $\{w_i\}_{i=0}^{n_w}$,

```
1: Minimum computational cost  $c^* \leftarrow +\infty$ 
2: for  $g_s = \max_i \{w_i\}_{i=1}^{n_w}$  to  $\sum_{i=1}^{n_w} w_i$  do
3:   Remaining windows  $\Phi \leftarrow \{w_i\}_{i=1}^{n_w}$ ; partition  $\Pi \leftarrow \emptyset$ ; the number of group  $n_g \leftarrow 0$ 
4:   repeat
5:      $\pi_{n_g} \leftarrow \text{Knapsack}(g_s, \Phi)$ , as in Equation (7)
6:      $\Pi \leftarrow \Pi \cup \pi_{n_g}$ ;  $\Phi \leftarrow \Phi \setminus \pi_{n_g}$ 
7:      $n_g \leftarrow n_g + 1$ 
8:   until  $\Phi = \emptyset$ 
9:    $c \leftarrow \mathcal{C}(g_s, \Pi)$ , as in Equation (8)
10:  if  $c < c^*$  then
11:     $c^* \leftarrow c$ ;  $\Pi^* \leftarrow \Pi$ 
12:  end if
13: end for
14: return Optimal group partition  $\Pi^*$ 
```

3.3 Optimal Grouping with Dynamic Programming

General formulation. The first step of the optimal grouping is to find an indexes partition Π with respect to the group size g_s :

$$\Pi = \{\pi_j\}_{j=1}^{n_g}, \quad (2)$$

$$s.t. \cup_j \pi_j = \{1, \dots, \sum_i w_i\}, \sum_j |\pi_j| = \sum_i w_i, \text{ and } \forall_j \sum_{k \in \pi_j} w_k \leq g_s. \quad (3)$$

where n_g is the number of resulting groups. The conditions in Equation (3) constrain the partition to contain all local windows with no duplicate and enforce the actual size of each group to be smaller than g_s . Based on the partition Π , we obtain a set of grouped tokens $\{\bar{\mathbf{X}}_j\}_{j=1}^{n_g}$ that

$$\bar{\mathbf{X}}_j = \text{Concat}(\{\hat{\mathbf{X}}_k : \forall k \in \pi_j\}), \bar{\mathbf{X}}_j \in \mathbb{R}^{C \times g_s},^2 \quad (4)$$

upon which the Masked Attention is performed. Finally, we apply the inverse operation of the partition Π to recover the positions of output tokens.

With the formulation above, there remain two questions unresolved: 1) how to choose the optimal group size g_s^* , and 2) how to obtain the optimal partition Π^* given g_s^* . To this end, we formulate our objectives as the below min-min optimization problem,

$$g_s^* = \operatorname{argmin}_{g_s} \mathcal{C}(g_s, \text{Partition}(g_s, \{w_i\}_i)), \quad (5)$$

$$\text{Partition}(g_s, \{w_i\}_{n_w}) = \operatorname{argmin}_{\Pi} |\Pi|, s.t. \text{ Equation (3)}, \quad (6)$$

where $\mathcal{C}(\cdot)$ is a cost function measuring the computation cost of the attention with the grouped tokens. Intuitively, Equation (5) aims to find the optimal group size g_s^* that the computation cost of the optimal partition w.r.t. g_s^* is the minimum. Equation (6) searches for the optimal partition, with the constraints of Equation (3). Having the optimal group size, we can directly obtain the optimal partition $\Pi^* = \text{Partition}(g_s^*, \{w_i\}_{n_w})$. Next, we will present in detail how we solve the above optimization problem.

Group partition with Dynamic Programming. We find that the optimization problem in Equations (6) and (3) is a special case of the multiple subset sum problem with identical capacities (MSSP-I), a variant of the well-known 0-1 multiple knapsack problem with identical capacities (MKP-I) [34, Chapter 10]. In our case, the group size is analogous to the capacity of knapsacks, the numbers of visible tokens $\{w_i\}_{n_w}$ are analogous to the values of goods, the weights of goods are the same as their values, and the number of knapsacks is unbounded. Although the general multiple knapsacks problem is NP-complete, its variant MSSP-I can be solved in pseudo-polynomial time

²Here we assume the number of tokens $\sum_i w_i$ is divisible by g_s for simplicity. In practice, we pad the group π_j when $|\pi_j|$ is smaller than g_s .

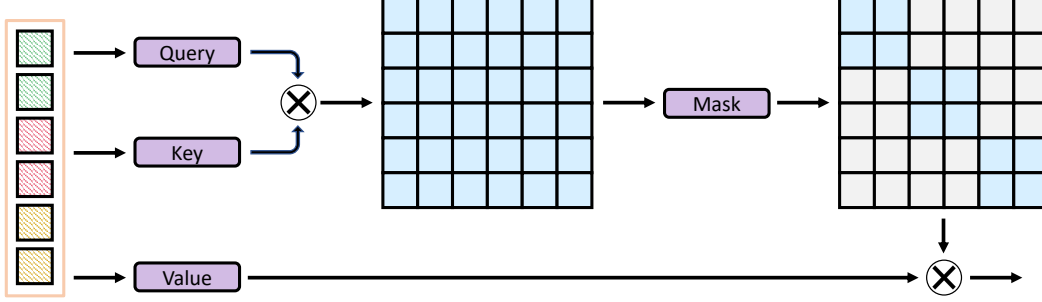


Figure 3: **Illustration of the Masked Attention scheme.** Given a group of tokens, we first compute their pairwise attention weights and then set the attention weights between tokens from different local windows to $-\infty$ (indicated by the gray cells). The final attention output is then computed with the masked attention map.

using the dynamic programming (DP) algorithms [4], owing to the identical capacities. Specifically, we make use of the DP algorithm for the single knapsack problem (or the subset sum problem):

$$\pi \leftarrow \text{Knapsack}(g_s, \Phi), \quad (7)$$

which selects a subset π that $\sum_{u \in \pi} |u| \leq g_s$ out of the full set Φ (the pseudo-code of this algorithm is given in Appendix). We alternatively apply this algorithm to the remaining full set Φ and exclude the selected subset π from Φ , until Φ is empty. In practice, we found that our algorithm is very fast and the time cost is negligible because the number of local windows is often small, *e.g.*, less than 100 in our pre-training stage.

Cost function. Because we mainly care about the efficiency, we use the FLOPs to measure the computation complexity of the multi-head attention on grouped tokens, *i.e.*,

$$\mathcal{C}(g_s, \Pi) = |\Pi| \times (4g_s C^2 + 2g_s^2 C) = n_g \times (4g_s C^2 + 2g_s^2 C), \quad (8)$$

where C is the number of channels. Although the complexity is quadratic w.r.t. the group size g_s , using smaller g_s might produce more groups (and more padding) and suffers from suboptimal efficiency. Therefore the optimal group size is determined adaptively during training.

Putting everything together. We sweep over the possible values of group size, from $\max_i w_i$ to $\sum_i w_i$, to find the optimal group size. For each selected group size, we firstly use the DP algorithm in Equation (7) to partition the windows and then calculate the computation cost of the attention this partition. The one with minimum cost is chosen as the optimal group size. The pseudo-code of the optimal grouping is summarized in Algorithm 1.

3.4 Masked Attention

Because non-adjacent local windows are partitioned into the same groups, masking the attention weights is needed to avoid the information exchange between these local windows. As illustrated in Figure 3, having computed the attention map, we retain only the intra-window attention weights (*i.e.*, the block-diagonal elements) and discard the inter-window ones. A similar masking scheme is also applied to the retrieving of relative position bias [43], where we store the original absolute position of each token and compute the relative positions on-the-fly to retrieve the corresponding biases.

3.5 Batch-wise Random Masking

We observed that the per-sample random masking strategy would deteriorate the efficiency of our method: 1) it might produce different numbers of groups of local windows for each sample, which is intractable for the parallel computation of the Masked Attention; 2) when the mask patch size is smaller than the largest patch size of the hierarchical models, some patches might contain both visible and masked inputs. In this case, we can not discard such patches during training and fail to fully take advantage of the sparsification. Therefore, we propose to set the mask patch size to the same value as the largest patch size of the encoder (*e.g.*, 32 for most hierarchical models, which is also the default choice of [66]) and use the same random mask for all samples in the same GPU device (*a.k.a.*, a micro-batch).

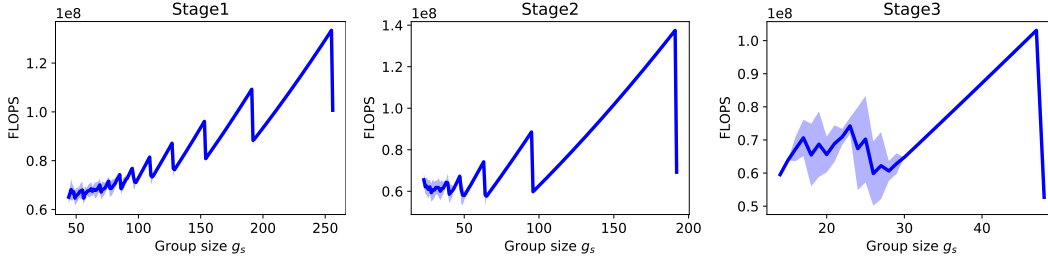


Figure 4: **The optimal group size g_s at each stage.** The figure of the fourth stage is omitted here because there is only one local window in this stage, so the grouping is not necessary. The simulation is repeated 100 times, of which the mean and standard deviation (the shaded regions) are reported.

4 Experiments

4.1 Implementation Details and Experimental Setups

We conduct experiments on the ImageNet-1K [54] (BSD 3-Clause License) image classification dataset and MS-COCO [41] (CC BY 4.0 License) object detection/instance segmentation dataset. The Swin-Base and Swin-Large [43] models, which consist of four stages with features of stride 4/8/16/32, are used as the encoder throughout this paper for direct comparisons with the baseline [66]. The model is first pre-trained on the ImageNet-1K dataset without label and then fine-tuned on downstream tasks. All the experiments of our method are performed on a single machine with eight 32G Tesla V100 GPUs, CUDA 10.1, PyTorch [48] 1.8, and automatic mixed-precision training [45].

Pre-training setup. We patchify images of size 224×224 with a patch size of 4×4 and randomly mask the patches with a ratio r ($r = 0.75$ by default) following the scheme in Section 3.5. The input images are transformed by a set of simple data augmentations, including random cropping and horizontal flip, and standardization. Following the prior work MAE [22], we use a lightweight decoder that consists of n_d (by default $n_d = 1$) transformer blocks with an embedding dimension of 512. The decoder takes the representations of visible patches and the mask token as input and is appended after the final stage of the encoder to learning representations for the masked patches. It is followed by a linear layer to predict the normalized pixel values of the masked patches. The models are trained for 100/200/400/800 epochs with a batch size of 2,048. We use the AdamW optimizer [35] with the cosine annealing schedule [44]. We set the base learning rate to $1.5e^{-4}$, weight decay to 0.05, the hyper-parameters of Adam $\beta_1 = 0.9$, $\beta_2 = 0.999$, the number of warmup epochs to 40 with an initial base learning rate $1.5e^{-7}$. The effective learning rate is scaled linearly by $\text{batch_size}/256$.

Fine-tuning on the ImageNet-1K dataset. For fine-tuning, we drop the decoder and directly append a 1,000-way fully-connected layer to the average-pooled output of the encoder as the classifier. The models are also optimized by the AdamW optimizer [35] with 100 training epochs in total, 20 warmup epochs, a base/warmup learning rate of $1.25e^{-4}/2.5e^{-7}$, the cosine annealing schedule [44], a weight decay of 0.05, a layerwise learning rate decay [2] of 0.9, and a stochastic depth [28] ratio of 0.1. The data augmentations are the same as [2, 66].

Fine-tuning on the MS-COCO dataset. We adopt the Mask R-CNN [24] architecture with the FPN [40] as the detector. All models are fine-tuned on the MS-COCO [41] 2017 train split ($\sim 118k$ images) and finally evaluated on the val split ($\sim 5k$ images). We use a batch size of 16, AdamW optimizer [35] with a learning rate of $1e^{-4}$, a weight decay of 0.05. The $1 \times /3 \times$ schedule in the mmdetection [8] is adopted, which uses 12/36 training epochs in total and decays the learning rate at the $\frac{3}{4}$ and $\frac{11}{12}$ of the total epochs by a factor of 10. The standard COCO metrics, including AP, AP₅₀, and AP₇₅ for both object detection and instance segmentation are used for evaluation.

4.2 Ablations studies

Efficiency comparison with SimMIM. We compare the efficiency of our method to the baseline SimMIM in Figure 1. The evaluations are performed on a single machine with eight 32GB V100 GPUs for our method and on 2 or 4 machines for the SimMIM because it fails to fit into a single machine with the default batch size of the original paper [66] (*i.e.*, 2,048). As we can see from the figures, the training of SimMIM with images of size 224^2 is very slow and memory-hungry. Although training with smaller images considerably reduces the training time and memory consumption, it still far lags behind our method with images of size 224^2 . Concretely, with the same amount of

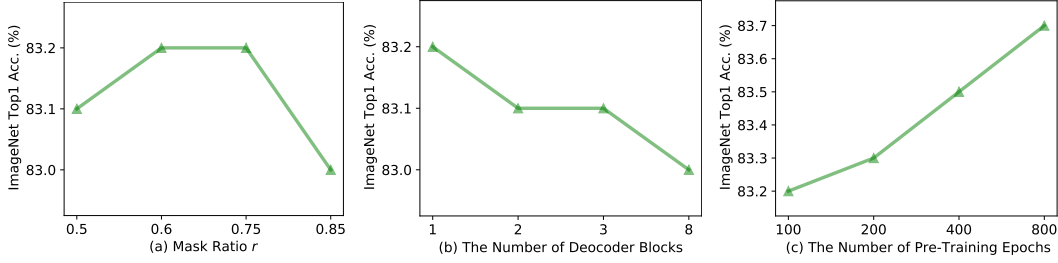


Figure 5: **Ablation studies of** (a) the choice of the mask ratio r , (b) the number of transformer blocks n_d in the decoder, and (c) the number of pre-training epochs.

training epochs, our method performs on par with baseline with $\sim 2\times$ speedup and $\sim 60\%$ of memory reduction using Swin-B. We also observe that the efficiency improvements become larger with the larger Swin-L, *e.g.*, $2.7\times$ speedup compared with SimMIM₁₉₂, highlighting the efficiency of our method with larger models.

The optimal group size g_s on each stage. Because hierarchical models have multiple stages with different scales of features, the optimal group size of each stage might also be different. Regarding this, we design a simulation experiment to analyze the optimal g_s at different stages. In the simulation, we randomly generate 100 masks following Section 3.5, compute the costs w.r.t. different choices of g_s , and report the mean/standard deviation of the costs in Figure 4. Note that the analysis of the 4th stage is omitted here because it only has one local window. In general, we observed that the cost increases quadratically w.r.t. the group size, except for some cases where group size is exactly equal to the sum of a subset of local windows. Another intriguing observation is that the cost at each stage seems to be the minimum around the point that $g_s = 49$, which is equal to the window size of the window attention. This observation indicates that we may not need to sweep over all possible group sizes but simply set $g_s = p \times p$ in practice.

The influence of the mask ratio, the number of decoder blocks, and the pre-training epochs.

From Figure 5(a), we can see that the performance of our method is quite stable with the mask ratio r varying from 0.5 to 0.85, which conforms with the observation of [22]. In Figure 5(b), we also study the influence of the depth of the decoder. Intriguingly, the results suggest that fewer decoder blocks produce better results. This study favors the simple prediction head design of SimMIM [66] with hierarchical models and is in contrast to the observation of MAE [22] with isotropic ones. For simplicity and efficiency, we fix $r = 0.75$ and the number of decoder blocks to 1 throughout the paper. Furthermore, we study the impact of pre-training budgets on our method. As shown in Figure 5(c), the fine-tuning accuracy increases steadily w.r.t. the number of training epochs and does not seem to stagnate, suggesting its potential for a further performance boost.

Pre-training with larger window size. The work of [42] puts forth that using a larger window size is beneficial for fine-tuning. In practice, however, it might be less practical because of the quadratic complexity of self-attention w.r.t. the window size. Fortunately, operating only on the visible patches permits the training with a larger window size with little extra cost. As displayed in Table 1, pre-training with doubled window size only marginally increases the training time/GPU memory by less than 10%/20% yet brings a moderate performance improvement despite $p = 7$ in the fine-tuning.

Table 1: A larger window size $p \times p$.

$p \times p$	Time	Mem.	Acc.
7×7	1.1h	121.6G	83.2%
14×14	1.2h	148.9G	83.4%

4.3 ImageNet-1K Classification

We fine-tune the pre-trained models on the ImageNet validation set and report the results in Table 2. Here, we make direct comparisons with the models 1) trained from scratch with a longer training schedule, 2) trained with contrastive learning, and 3) trained with MIM. Our approach achieves 83.7% top-1 fine-tuning accuracy with the Swin-Base backbone, which is superior to the supervised learning/contrastive learning methods and on par with other MIM methods using backbones with similar capacities. The results demonstrate the effectiveness of our method, in addition to the substantial efficiency improvements over both MAE and SimMIM. The experiments with the Swin-L backbone are given in Appendix to have a further inspection on our method.

Table 2: Top1 accuracy on the ImageNet-1K validation set with the Swin-B or ViT-B models. All methods are trained with images of size 224×224 in both the pre-training and fine-tuning except for SimMIM₁₉₂ using 192×192 in the pre-training.

Method	Model	#Params	PT Ep.	Ep. Hours	Total Hours	FT Ep.	Acc. (%)
<i>Training from scratch</i>							
Scratch, DeiT [56]	ViT-B	86M	0	-	-	300	81.8
Scratch, MAE [22]	ViT-B	86M	0	-	-	300	82.3
Scratch, Swin [43]	Swin-B	88M	0	-	-	300	83.5
<i>Supervised Pre-training</i>							
Supervised, SimMIM [66]	Swin-B	88M	300	-	-	100	83.3
Supervised, SimMIM [66]	Swin-L	197M	300	-	-	100	83.5
<i>Pre-training with Contrastive Learning</i>							
MoCov3 [11]	ViT-B	86M	800	-	-	100	83.2
DINO [7]	ViT-B	86M	800	-	-	100	82.8
<i>Pre-training with Masked Image Modeling</i>							
BEiT [2]	ViT-B	86M	800	-	-	100	83.2
MaskFeat [62]	ViT-B	86M	800	-	-	100	84.0
MAE [22]	ViT-B	86M	1600	1.3	2069	100	83.6
SimMIM ₂₂₄ [66]	ViT-B	86M	800	4.1	3307	100	83.8
SimMIM ₁₉₂ [66]	Swin-B	88M	800	2.0	1609	100	84.0
SimMIM ₁₉₂ [66]	Swin-L	197M	800	3.5	2821	100	85.4
Ours	Swin-B	88M	800	1.1	887	100	83.7
Ours	Swin-L	197M	800	1.3	1067	100	85.1

Table 3: **MS-COCO object detection and instance segmentation.** All methods are based on the Mask R-CNN [24] architecture with the FPN [40] neck. The methods in gray are cited from [39]. Most of them use much longer training schedules and advanced data augmentations.

Method	Backbone	PT Ep.	PT Hours	FT Epochs	AP ^b	AP ₅₀ ^b	AP ₇₅ ^b	AP ^m	AP ₅₀ ^m	AP ₇₅ ^m
<i>Training from scratch</i>										
Benchmarking [39]	ViT-B	0	0	400	48.9	-	-	43.6	-	-
<i>Supervised Pretraining</i>										
Benchmarking [39]	ViT-B	300	992	100	47.9	-	-	42.9	-	-
PVT [60]	PVT-L	300	-	36	44.5	66.0	48.3	40.7	63.4	43.7
Swin [43]	Swin-B	300	840	36	48.5	69.8	53.2	43.2	66.9	46.7
<i>Self-Supervised Pre-training</i>										
MoCov3 [11]	ViT-B	800	-	100	47.9	-	-	42.7	-	-
BEiT [2]	ViT-B	800	-	100	49.8	-	-	44.4	-	-
MAE [22]	ViT-B	1600	2069	25	48.1	-	-	-	-	-
MAE [22]	ViT-B	1600	2069	100	50.3	-	-	44.9	-	-
SimMIM [66]	Swin-B	800	1609	36	50.4	70.9	55.5	44.4	68.2	47.9
Ours	Swin-B	800	887	36	50.0	70.7	55.4	44.1	67.9	47.5

4.4 MS-COCO Object Detection and Instance Segmentation

Finally, we evaluate the transfer learning performance of our pre-trained models to the MS-COCO object detection and instance segmentation dataset. Here, we directly use the code base of the supervised Swin Transformer without any modification to the fine-tuning strategy. For direct comparisons, we reran the experiments for the supervised Swin-B and SimMIM using their public checkpoints. The experiment results are summarized in Table 3. Compared with the supervised pre-trained Swin-B, our approach performs prominently better in terms of all metrics, *e.g.*, 1.5% absolute improvement in AP^b. In addition, we also observed that our approach still performs comparably to the SimMIM on dense prediction tasks. More significantly, our approach outperforms most of the baselines from [39] using $3\times$ or $10\times$ more fine-tuning epochs and advanced data augmentations [17]. These experiments, combined with the results in Table 2, verify that our approach can achieve outstanding performance with impressive pre-training efficiency.

5 Conclusion

In this paper, we present a **green** approach for Masked Image Modeling (MIM) with hierarchical Vision Transformers, *e.g.*, Swin Transformer [43], allowing the hierarchical models to discard masked patches and operate only on the visible ones. Coupling the efficient Group Window Attention scheme and the DP-algorithm-based Optimal Grouping strategy, our approach can train the hierarchical models $\sim 2.7\times$ faster and reduce the GPU memory consumption by 70%, while still enjoying a competitive performance on ImageNet classification and the superiority of downstream MS-COCO object detection benchmarks. We hope that this work will facilitate future self-supervised learning methods targeting both effectiveness and efficiency.

Limitations. One of the limitations of our algorithm is that it requires the batch-wise masking scheme (as in Section 3.5) to achieve the best efficiency. Although this limitation only has little impact on the MIM pre-training, it restrains the application of our method on a broader range of settings, *e.g.*, training ViTs with token sparsification [53, 68] that requires instance-wise sparsification. These applications are beyond the scope of this work and we will leave them for the future study.

Broader Impact. This work proposed a green approach for MIM with hierarchical ViTs, prominently alleviating the heavy computation burden of MIM. On the one hand, this work provokes the efficiency as well as the effectiveness of MIM, which may inspire new algorithms and investigations on this direction. On the other hand, since the pre-training datasets might contain biases, our approach, in the same way as other unsupervised/self-supervised learning methods, might also be susceptible to replicate these biases. This concern can be mitigated by combining the FairML methods [3].

References

- [1] A. Baevski, W.-N. Hsu, Q. Xu, A. Babu, J. Gu, and M. Auli. Data2vec: A general framework for self-supervised learning in speech, vision and language. *arXiv preprint arXiv:2202.03555*, 2022.
- [2] H. Bao, L. Dong, and F. Wei. Beit: Bert pre-training of image transformers. *arXiv preprint arXiv:2106.08254*, 2021.
- [3] S. Barocas, M. Hardt, and A. Narayanan. Fairness in machine learning. *Nips tutorial*, 1:2, 2017.
- [4] R. Bellman. Dynamic programming. *Science*, 153(3731):34–37, 1966.
- [5] T. B. Brown, B. Mann, N. Ryder, M. Subbiah, J. Kaplan, P. Dhariwal, A. Neelakantan, P. Shyam, G. Sastry, A. Askell, et al. Language models are few-shot learners. In *Advances in Neural Information Processing Systems*, volume 33, 2020.
- [6] M. Caron, I. Misra, J. Mairal, P. Goyal, P. Bojanowski, and A. Joulin. Unsupervised learning of visual features by contrasting cluster assignments. *Advances in Neural Information Processing Systems*, 33, 2020.
- [7] M. Caron, H. Touvron, I. Misra, H. Jégou, J. Mairal, P. Bojanowski, and A. Joulin. Emerging properties in self-supervised vision transformers. *arXiv preprint arXiv:2104.14294*, 2021.
- [8] K. Chen, J. Wang, J. Pang, Y. Cao, Y. Xiong, X. Li, S. Sun, W. Feng, Z. Liu, J. Xu, et al. Mmdetection: Open mmlab detection toolbox and benchmark. *arXiv preprint arXiv:1906.07155*, 2019.
- [9] T. Chen, S. Kornblith, M. Norouzi, and G. Hinton. A simple framework for contrastive learning of visual representations. In *International Conference on Machine Learning*, 2020.
- [10] X. Chen and K. He. Exploring simple Siamese representation learning. *arXiv preprint arXiv:2011.10566*, 2020.
- [11] X. Chen, S. Xie, and K. He. An empirical study of training self-supervised vision transformers. In *Proceedings of the IEEE/CVF International Conference on Computer Vision*, pages 9640–9649, 2021.
- [12] X. Chu, Z. Tian, Y. Wang, B. Zhang, H. Ren, X. Wei, H. Xia, and C. Shen. Twins: Revisiting the design of spatial attention in vision transformers. *Advances in Neural Information Processing Systems*, 34, 2021.
- [13] J. Devlin, M.-W. Chang, K. Lee, and K. Toutanova. Bert: Pre-training of deep bidirectional transformers for language understanding. In *North American Chapter of the Association for Computational Linguistics: Human Language Technologies*, pages 4171–4186, 2019.
- [14] X. Dong, J. Bao, T. Zhang, D. Chen, W. Zhang, L. Yuan, D. Chen, F. Wen, and N. Yu. Peco: Perceptual codebook for bert pre-training of vision transformers. *arXiv preprint arXiv:2111.12710*, 2021.
- [15] A. Dosovitskiy, L. Beyer, A. Kolesnikov, D. Weissenborn, X. Zhai, T. Unterthiner, M. Dehghani, M. Minderer, G. Heigold, S. Gelly, et al. An image is worth 16x16 words: Transformers for image recognition at scale. *arXiv preprint arXiv:2010.11929*, 2020.

- [16] H. Fan, B. Xiong, K. Mangalam, Y. Li, Z. Yan, J. Malik, and C. Feichtenhofer. Multiscale vision transformers. In *Proceedings of the IEEE/CVF International Conference on Computer Vision*, pages 6824–6835, 2021.
- [17] G. Ghiasi, Y. Cui, A. Srinivas, R. Qian, T.-Y. Lin, E. D. Cubuk, Q. V. Le, and B. Zoph. Simple copy-paste is a strong data augmentation method for instance segmentation. In *Proceedings of the IEEE/CVF Conference on Computer Vision and Pattern Recognition*, pages 2918–2928, 2021.
- [18] S. Gidaris, P. Singh, and N. Komodakis. Unsupervised representation learning by predicting image rotations. In *International Conference on Learning Representation*, 2018.
- [19] R. Girshick, J. Donahue, T. Darrell, and J. Malik. Rich feature hierarchies for accurate object detection and semantic segmentation. In *IEEE Conference on Computer Vision and Pattern Recognition*, pages 580–587, 2014.
- [20] I. Goodfellow, J. Pouget-Abadie, M. Mirza, B. Xu, D. Warde-Farley, S. Ozair, A. Courville, and Y. Bengio. Generative adversarial nets. In *Advances in Neural Information Processing Systems*, pages 2672–2680, 2014.
- [21] J.-B. Grill, F. Strub, F. Altché, C. Tallec, P. Richemond, E. Buchatskaya, C. Doersch, B. Avila Pires, Z. Guo, M. Gheshlaghi Azar, et al. Bootstrap your own latent: A new approach to self-supervised learning. *Advances in Neural Information Processing Systems*, 33, 2020.
- [22] K. He, X. Chen, S. Xie, Y. Li, P. Dollár, and R. Girshick. Masked autoencoders are scalable vision learners. *arXiv preprint arXiv:2111.06377*, 2021.
- [23] K. He, H. Fan, Y. Wu, S. Xie, and R. Girshick. Momentum contrast for unsupervised visual representation learning. In *IEEE Conference on Computer Vision and Pattern Recognition*, pages 9729–9738, 2020.
- [24] K. He, G. Gkioxari, P. Dollár, and R. Girshick. Mask r-cnn. In *Proceedings of the IEEE international conference on computer vision*, pages 2961–2969, 2017.
- [25] K. He, X. Zhang, S. Ren, and J. Sun. Deep residual learning for image recognition. In *IEEE Conference on Computer Vision and Pattern Recognition*, pages 770–778, 2016.
- [26] O. J. Hénaff, S. Koppula, J.-B. Alayrac, A. v. d. Oord, O. Vinyals, and J. Carreira. Efficient visual pretraining with contrastive detection. *arXiv preprint arXiv:2103.10957*, 2021.
- [27] J. Ho, A. Jain, and P. Abbeel. Denoising diffusion probabilistic models. *Advances in Neural Information Processing Systems*, 33:6840–6851, 2020.
- [28] G. Huang, Y. Sun, Z. Liu, D. Sedra, and K. Q. Weinberger. Deep networks with stochastic depth. In *European Conference on Computer Vision*, pages 646–661. Springer, 2016.
- [29] L. Huang, S. You, M. Zheng, F. Wang, C. Qian, and T. Yamasaki. Learning where to learn in cross-view self-supervised learning. *arXiv preprint arXiv:2203.14898*, 2022.
- [30] L. Huang, Y. Yuan, J. Guo, C. Zhang, X. Chen, and J. Wang. Interlaced sparse self-attention for semantic segmentation. *arXiv preprint arXiv:1907.12273*, 2019.
- [31] L. Huang, C. Zhang, and H. Zhang. Self-adaptive training: Bridging supervised and self-supervised learning. *arXiv preprint arXiv:2101.08732*, 2021.
- [32] Z. Huang, Y. Ben, G. Luo, P. Cheng, G. Yu, and B. Fu. Shuffle transformer: Rethinking spatial shuffle for vision transformer. *arXiv preprint arXiv:2106.03650*, 2021.
- [33] T. Karras, S. Laine, and T. Aila. A style-based generator architecture for generative adversarial networks. In *Proceedings of the IEEE/CVF conference on computer vision and pattern recognition*, pages 4401–4410, 2019.
- [34] H. Kellerer, U. Pferschy, and D. Pisinger. *Knapsack problems*. Springer, 2004.
- [35] D. P. Kingma and J. Ba. Adam: A method for stochastic optimization. In *International Conference on Learning Representations*, 2015.
- [36] D. P. Kingma and M. Welling. Auto-encoding variational Bayes. In *International Conference on Learning Representations*, 2014.
- [37] A. Krizhevsky, I. Sutskever, and G. E. Hinton. Imagenet classification with deep convolutional neural networks. In *Advances in Neural Information Processing Systems*, volume 25, pages 1097–1105, 2012.
- [38] G. Larsson, M. Maire, and G. Shakhnarovich. Colorization as a proxy task for visual understanding. In *Proceedings of the IEEE conference on computer vision and pattern recognition*, pages 6874–6883, 2017.
- [39] Y. Li, S. Xie, X. Chen, P. Dollar, K. He, and R. Girshick. Benchmarking detection transfer learning with vision transformers. *arXiv preprint arXiv:2111.11429*, 2021.
- [40] T.-Y. Lin, P. Dollár, R. Girshick, K. He, B. Hariharan, and S. Belongie. Feature pyramid networks for object detection. In *Proceedings of the IEEE conference on computer vision and pattern recognition*, pages 2117–2125, 2017.

- [41] T.-Y. Lin, M. Maire, S. Belongie, J. Hays, P. Perona, D. Ramanan, P. Dollár, and C. L. Zitnick. Microsoft coco: Common objects in context. In *European conference on computer vision*, pages 740–755. Springer, 2014.
- [42] Z. Liu, H. Hu, Y. Lin, Z. Yao, Z. Xie, Y. Wei, J. Ning, Y. Cao, Z. Zhang, L. Dong, et al. Swin transformer v2: Scaling up capacity and resolution. *arXiv preprint arXiv:2111.09883*, 2021.
- [43] Z. Liu, Y. Lin, Y. Cao, H. Hu, Y. Wei, Z. Zhang, S. Lin, and B. Guo. Swin transformer: Hierarchical vision transformer using shifted windows. In *Proceedings of the IEEE/CVF International Conference on Computer Vision*, pages 10012–10022, 2021.
- [44] I. Loshchilov and F. Hutter. SGDR: Stochastic gradient descent with warm restarts. In *International Conference on Learning Representations*, 2017.
- [45] P. Micikevicius, S. Narang, J. Alben, G. Diamos, E. Elsen, D. Garcia, B. Ginsburg, M. Houston, O. Kuchaiev, G. Venkatesh, et al. Mixed precision training. *arXiv preprint arXiv:1710.03740*, 2017.
- [46] M. Noroozi and P. Favaro. Unsupervised learning of visual representations by solving jigsaw puzzles. In *European Conference on Computer Vision*, pages 69–84. Springer, 2016.
- [47] A. v. d. Oord, Y. Li, and O. Vinyals. Representation learning with contrastive predictive coding. *arXiv preprint arXiv:1807.03748*, 2018.
- [48] A. Paszke, S. Gross, F. Massa, A. Lerer, J. Bradbury, G. Chanan, T. Killeen, Z. Lin, N. Gimelshein, L. Antiga, et al. Pytorch: An imperative style, high-performance deep learning library. In *Advances in Neural Information Processing Systems*, pages 8024–8035, 2019.
- [49] D. Pathak, P. Krahenbuhl, J. Donahue, T. Darrell, and A. A. Efros. Context encoders: Feature learning by inpainting. In *IEEE Conference on Computer Vision and Pattern Recognition*, pages 2536–2544, 2016.
- [50] A. Radford, K. Narasimhan, T. Salimans, and I. Sutskever. Improving language understanding by generative pre-training, 2018.
- [51] A. Radford, J. Wu, R. Child, D. Luan, D. Amodei, and I. Sutskever. Language models are unsupervised multitask learners. *OpenAI blog*, 1(8):9, 2019.
- [52] A. Ramesh, M. Pavlov, G. Goh, S. Gray, C. Voss, A. Radford, M. Chen, and I. Sutskever. Zero-shot text-to-image generation. In *International Conference on Machine Learning*, pages 8821–8831. PMLR, 2021.
- [53] Y. Rao, W. Zhao, B. Liu, J. Lu, J. Zhou, and C.-J. Hsieh. Dynamicvit: Efficient vision transformers with dynamic token sparsification. *Advances in neural information processing systems*, 34, 2021.
- [54] O. Russakovsky, J. Deng, H. Su, J. Krause, S. Satheesh, S. Ma, Z. Huang, A. Karpathy, A. Khosla, M. Bernstein, et al. Imagenet large scale visual recognition challenge. *International Journal of Computer Vision*, 115(3):211–252, 2015.
- [55] R. Schwartz, J. Dodge, N. A. Smith, and O. Etzioni. Green ai. *Communications of the ACM*, 63(12):54–63, 2020.
- [56] H. Touvron, M. Cord, M. Douze, F. Massa, A. Sablayrolles, and H. Jégou. Training data-efficient image transformers & distillation through attention. In *International Conference on Machine Learning*, pages 10347–10357. PMLR, 2021.
- [57] A. Van Den Oord, O. Vinyals, et al. Neural discrete representation learning. *Advances in neural information processing systems*, 30, 2017.
- [58] A. Vaswani, N. Shazeer, N. Parmar, J. Uszkoreit, L. Jones, A. N. Gomez, Ł. Kaiser, and I. Polosukhin. Attention is all you need. *Advances in neural information processing systems*, 30, 2017.
- [59] P. Vincent, H. Larochelle, Y. Bengio, and P.-A. Manzagol. Extracting and composing robust features with denoising autoencoders. In *International Conference on Machine Learning*, pages 1096–1103, 2008.
- [60] W. Wang, E. Xie, X. Li, D.-P. Fan, K. Song, D. Liang, T. Lu, P. Luo, and L. Shao. Pyramid vision transformer: A versatile backbone for dense prediction without convolutions. In *Proceedings of the IEEE/CVF International Conference on Computer Vision*, pages 568–578, 2021.
- [61] X. Wang, R. Zhang, C. Shen, T. Kong, and L. Li. Dense contrastive learning for self-supervised visual pre-training. In *Proceedings of the IEEE/CVF Conference on Computer Vision and Pattern Recognition*, pages 3024–3033, 2021.
- [62] C. Wei, H. Fan, S. Xie, C.-Y. Wu, A. Yuille, and C. Feichtenhofer. Masked feature prediction for self-supervised visual pre-training. *arXiv preprint arXiv:2112.09133*, 2021.
- [63] Z. Wu, Y. Xiong, S. X. Yu, and D. Lin. Unsupervised feature learning via non-parametric instance discrimination. In *IEEE Conference on Computer Vision and Pattern Recognition*, pages 3733–3742, 2018.
- [64] T. Xiao, C. J. Reed, X. Wang, K. Keutzer, and T. Darrell. Region similarity representation learning. *arXiv preprint arXiv:2103.12902*, 2021.

- [65] Z. Xie, Y. Lin, Z. Zhang, Y. Cao, S. Lin, and H. Hu. Propagate yourself: Exploring pixel-level consistency for unsupervised visual representation learning. In *Proceedings of the IEEE/CVF Conference on Computer Vision and Pattern Recognition*, pages 16684–16693, 2021.
- [66] Z. Xie, Z. Zhang, Y. Cao, Y. Lin, J. Bao, Z. Yao, Q. Dai, and H. Hu. Simmim: A simple framework for masked image modeling. *arXiv preprint arXiv:2111.09886*, 2021.
- [67] J. Xu, W. Zhou, Z. Fu, H. Zhou, and L. Li. A survey on green deep learning. *arXiv preprint arXiv:2111.05193*, 2021.
- [68] H. Yin, A. Vahdat, J. Alvarez, A. Mallya, J. Kautz, and P. Molchanov. Adavit: Adaptive tokens for efficient vision transformer. *arXiv preprint arXiv:2112.07658*, 2021.
- [69] Y. Yuan, R. Fu, L. Huang, W. Lin, C. Zhang, X. Chen, and J. Wang. Hrformer: High-resolution vision transformer for dense predict. *Advances in Neural Information Processing Systems*, 34, 2021.
- [70] J. Zbontar, L. Jing, I. Misra, Y. LeCun, and S. Deny. Barlow twins: Self-supervised learning via redundancy reduction. *arXiv preprint arXiv:2103.03230*, 2021.
- [71] M. Zheng, F. Wang, S. You, C. Qian, C. Zhang, X. Wang, and C. Xu. Weakly supervised contrastive learning. In *Proceedings of the IEEE/CVF International Conference on Computer Vision (ICCV)*, pages 10042–10051, October 2021.
- [72] M. Zheng, S. You, F. Wang, C. Qian, C. Zhang, X. Wang, and C. Xu. Rssl: Relational self-supervised learning with weak augmentation. *Advances in Neural Information Processing Systems*, 34, 2021.
- [73] J. Zhou, C. Wei, H. Wang, W. Shen, C. Xie, A. Yuille, and T. Kong. ibot: Image bert pre-training with online tokenizer. *arXiv preprint arXiv:2111.07832*, 2021.

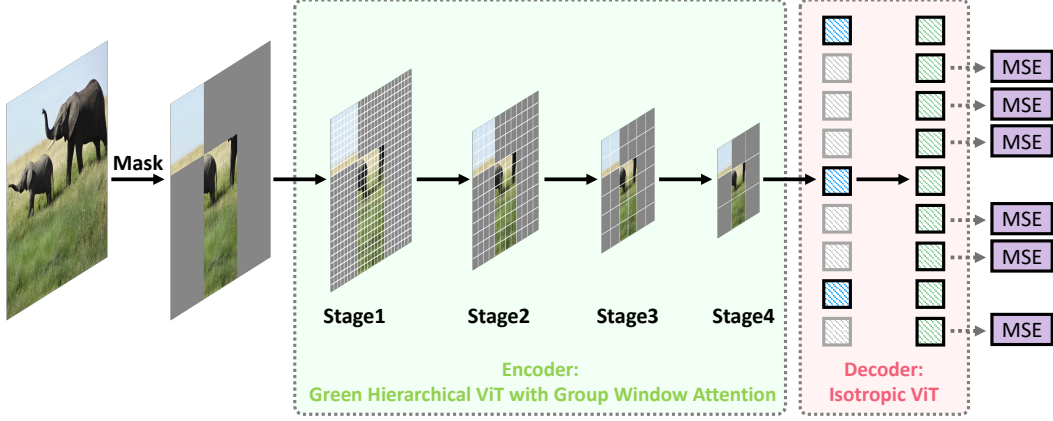


Figure 6: **Overview of our method.** The input image is randomly masked and then fed into a 4-stage hierarchical ViTs. Finally, a lightweight decoder takes the representations of visible patches and mask tokens to reconstruct the missing patches.

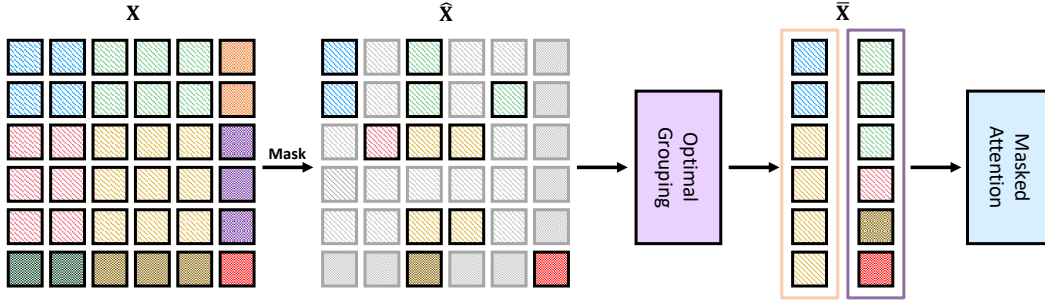


Figure 7: **Illustration of the Group Window Attention scheme with shifted windows.** It shows that our approach is agnostic to the window partition.

A More Details of Our Method

A.1 Method Overview.

We provide a diagram in Figure 6 for an intuitive illustration of our method. The input image is first randomly masked according to masking scheme in Section 3.5, then fed into our green hierarchical ViT to obtain representations for each visible patches. Finally, we concatenate the representations of visible patches with the mask tokens and feed them into a transformer decoder, yielding the representations for the masked patches. Finally, we predict the raw pixel values of masked patches from the corresponding representations and implement the training by minimizing the Mean Square Error (MSE) between the predictions and ground-truth.

A.2 Group Window Attention scheme with shifted windows.

In addition to Figure 2, we also illustrate how our method works with the irregular window partition in Figure 7. We can observe that, owing to the optimal grouping scheme, our method dynamically finds out the best group partition despite the numbers of visible patches within each local window is highly uneven. This figure further demonstrates that our approach is agnostic to the window partition and works impressively well.

Algorithm 2 Dynamic Programming-based algorithm for the Optimal Grouping using Python.

```
1 def Knapsack(g_s, Phi):
2     # g_s (int): Group size
3     # Phi (list[int]): The numbers of visible patches within each local window
4
5     n_w = len(Phi) # the number of windows
6     K = [[0 for w in range(g_s + 1)] for i in range(n_w + 1)] # a buffer for the DP
        algorithm
7
8     # Build table K[][] in a bottom up manner
9     for i in range(n_w + 1):
10         for w in range(g_s + 1):
11             if i == 0 or w == 0:
12                 K[i][w] = 0
13             elif Phi[i - 1] <= w:
14                 K[i][w] = max(Phi[i - 1] + K[i - 1][w - Phi[i - 1]], K[i - 1][w])
15             else:
16                 K[i][w] = K[i - 1][w]
17
18     # Store the result of Knapsack
19     res = K[n_w][g_s]
20
21     # Store the selected indexes
22     w = g_s
23     Pi = []
24
25     for i in range(n_w, 0, -1):
26         if res <= 0:
27             break
28
29         if res == K[i - 1][w]: # This window is not included.
30             continue
31         else: # This window is included.
32             Pi.append(i - 1)
33             # Since this window is included, its value is deducted
34             res = res - Phi[i - 1]
35             w = w - Phi[i - 1]
36
37     return Pi[::-1] # Optional: make Pi in an increasing order
38
39
40 def GroupPartition(g_s, Phi):
41     # g_s (int): Group size
42     # Phi (list[int]): The numbers of visible patches within each local window
43
44     win_szs = Phi.copy()
45     ori_win_idx = list(range(len(win_szs)))
46     win_idx = []
47
48     while len(win_szs) > 0:
49         idx = knapsack(group_size, win_szs)
50
51         # Append the selected idx
52         win_idx.append([ori_win_idx[i] for i in idx])
53
54         # The remaining windows and indexes
55         win_szs = [win_szs[i] for i in range(len(ori_win_idx)) if i not in idx]
56         ori_win_idx = [ori_win_idx[i] for i in range(len(ori_win_idx)) if i not in idx]
57
58     return win_idx
```

A.3 A Python Implementation of the Optimal Grouping algorithm

We provide a Python implementation of the Dynamic-Programming-based Optimal Grouping algorithm in Algorithm 2. As we can see, the two components of the Optimal Grouping algorithm are both easy to implement. For the DP algorithm for the single Knapsack problem, its time/space complexity is $\mathcal{O}(g_s n_w)$ where g_s is the group size and n_w is the number of windows. In practice, because g_s and n_w are generally small (*i.e.*, smaller than 100) the running time of Algorithm 2 is negligible (*i.e.*, $< 1\text{ms}$).

Algorithm 3 Group Attention using the PyTorch framework.

```
1 def GroupAttention(x, g_s, Phi):
2     # x (3-d tensor): Features the visible patches
3     # g_s (int): Group size
4     # Phi (list[int]): The numbers of visible patches within each local window
5
6     # B is the batch size, L is the number of visible patches, C is the number of channels
7     B, L, C = x.shape
8
9     # Prepare for the group attention
10    win_idx = GroupPartition(g_s, Phi)
11    patch_idx = torch.arange(sum(Phi))
12    patch_idx = torch.split(patch_idx, Phi)
13    shuffle_idx = torch.cat([patch_idx[wi] for wi in win_idx])
14    unshuffle_idx = torch.argsort(shuffle_idx)
15
16    # Group partition. For simplicity, assume that the partition is even
17    x = torch.index_select(x, 1, shuffle_idx) # (B, n_g * g_s, C)
18    x = x.reshape(-1, g_s, C) # (B * n_g, g_s, C)
19
20    # Attention with relative position bias as in Figure 3
21    x = MaskedAttention(x)
22
23    # Reverse the group partition
24    x = x.reshape(B, L, C).index_select(x, 1, unshuffle_idx)
25
26    return x
```

A.4 A PyTorch Implementation of the Group Attention scheme

With the group partition on the indexes, we can then permute visible patches according to the partition and obtain several groups of patches with a equal size g_s , upon which the Masked Attention is performed. We also provide a PyTorch implementation of the Group Attention scheme in Algorithm 3 to facilitate future research. Note the the padding operations is omitted here for simplicity.